

Prediction for the elastic modulus of polycrystalline materials: Theoretical derivation, verification, and application

Z. J. Zhang ^{1,2,*}, X. T. Li ^{3,†}, R. H. Li ⁴, R. Liu,^{1,2} Z. Qu,^{1,2} A. G. Sheinerman ⁵ and Z. F. Zhang ^{1,2,‡}

¹*Shi-changxu Innovation Center for Advanced Materials, Institute of Metal Research, Chinese Academy of Sciences, Shenyang 110016, China*

²*School of Materials Science and Engineering, University of Science and Technology of China, Shenyang 110016, China*

³*Institute for Advanced Study, Chengdu University, Chengdu 610106, China*

⁴*School of Mechanical Engineering, Liaoning Petrochemical University, Fushun 113001, China*

⁵*Institute of Problems of Mechanical Engineering, Russian Academy of Sciences, St. Petersburg 199178, Russia*



(Received 25 April 2023; revised 24 September 2023; accepted 2 November 2023; published 20 November 2023)

Based on our proposed layer-by-layer integrating method, the elastic modulus of an arbitrary inclined connection unit of two grains is derived. Furthermore, the derived formula is extended to the multibody connection of polycrystalline grains. Then, the derived formulae are verified by the finite element method and the experimental results available. Finally, an efficient software program is developed based on the derived formula to predict the elastic moduli of polycrystalline materials through the orientation measurement by electron backscatter diffraction, which is consistent with related experimental data. This work provides a simple method and software to predict accurately the elastic modulus of polycrystalline materials.

DOI: [10.1103/PhysRevB.108.174104](https://doi.org/10.1103/PhysRevB.108.174104)

I. INTRODUCTION

The elastic modulus is a crucial material parameter that is closely related to the deformation and fracture of materials, affecting the operational safety of engineering structures. Therefore, the research on the elastic modulus of materials has always been a popular field [1–10]. From a mechanical perspective, the elastic modulus can be regarded as the ability of materials to resist elastic deformation under applied loading, which is actually manifested at the atomic scale as the strength of the binding forces between atoms [11]. In fact, the elastic modulus not only determines the elastic deformation behavior, but also it affects plastic deformation and the fracture behaviors of materials [11–13]. For instance, the dislocation motion resistances (including Peierls-Nabarro stress and dislocation-interaction stress) and the energy associated with dislocation generation are both quantitatively related to the elastic modulus [12]. Additionally, the surface energy that must be overcome during the crack-growth process is directly proportional to the elastic modulus [11]. Thus, predicting the elastic modulus is of utmost importance for the analysis of mechanical properties of materials.

The mechanical properties of polycrystalline materials can be optimized and designed by adjusting their microstructures, such as grain size, grain-boundary structures, and second phases [14–18]. Therefore, polycrystalline materials are widely used in engineering structures. It is well known that polycrystalline materials consist of different grains with various orientations and grain boundaries [11, 19, 20]. The effect of

grain boundaries on the macroscopic elastic properties can be neglected when the coarse-grained materials are considered because the volume fraction of the grain boundary phase is very low [19, 20]. The elastic modulus of various grains with different orientations are quite different, and the macroscopic elastic properties of polycrystalline materials result from the aggregate of all the grains [21]. Therefore, this gives rise to an open question: how does one calculate the accurate elastic modulus of polycrystalline materials with multiple orientations in the component grains?

Several existing works have attempted to solve the aforesaid problem. Voigt [22] and Reuss [23] proposed the well-known approximation methods for evaluating the elastic modulus of multiphase materials. Their calculation formulae can be expressed as

$$E_c = \sum_{i=1}^n E_i V_i \text{Voigt approximation} \quad (1)$$

$$\frac{1}{E_c} = \sum_{i=1}^n \frac{V_i}{E_i} \text{Reuss approximation},$$

in which V_i is the volume fraction of the i th phase, E_i is the elastic modulus of the i th phase, and E_c is the elastic modulus of the composite. However, Voigt and Reuss approximations can only determine the upper and lower bounds for the elastic modulus of polycrystalline materials. Based on the formulae in Eq. (1), some modified methods were proposed to predict the elastic constants of the polycrystals [24–27]. Based on the variational principles, Hashin and Shtrikman [28] proposed a theoretical method to improve the calculation accuracy of Voigt and Reuss bounds. By considering a particular periodic arrangement of cubic inclusions and different connection sequences, Ravichandran [29] developed a method to predict the elastic modulus of two-phase composites, which showed a narrower limit than the method proposed by Hashin and Shtrikman [28]. While these modified methods offer certain

*zjzhang@imr.ac.cn

†lixiaotao@cdu.edu.cn

‡zhfzhang@imr.ac.cn

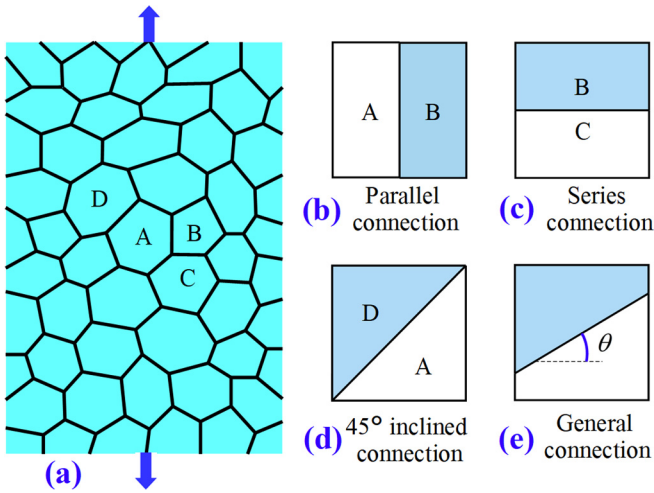


FIG. 1. The many-body connection of a polycrystal consists of various two-phase connections: (a) a polycrystal containing numerous grains with different orientations, (b) the parallel connection unit, (c) the series connection unit, (d) the 45° inclined connection unit, and (e) a general connection unit.

advantages over Voigt and Reuss approximations in terms of predicting the elastic modulus with higher accuracy, most of them tend to be more complex and difficult to apply. Furthermore, these methods can only provide upper and lower bounds for the effective elastic modulus of multiphase materials, rather than an exact value. To address this issue, this work proposes a theoretical method to calculate accurately the elastic modulus of polycrystalline materials and to develop a software program to predict the elastic modulus efficiently.

This work is organized as follows. In Sec. II, we propose the layer-by-layer integrating (LLI) method and derive the elastic modulus of an arbitrary inclined connection of two-phase materials, and then extend the solution to obtain the elastic modulus of polycrystalline materials. In Sec. III, two-dimensional bicrystal and three-dimensional polycrystalline finite element models are established to verify the formulae derived in Sec. II. In Sec. IV, an electron backscatter diffraction (EBSD)-based software program is developed to predict the elastic modulus of polycrystalline materials, and the predicted results are verified by the corresponding experiment data. Finally, in Sec. V, important conclusions are summarized.

II. METHODOLOGY

A. Problem description

For a polycrystal consisting of numerous crystals, as depicted in Fig. 1(a), Voigt and Reuss approximations assumed a parallel and a series connection unit of these crystals, respectively. However, the actual case is neither of them, but rather an intermediate case between them. To evaluate the elastic modulus of a polycrystal, two problems need to be addressed:

1. As the connection modes between two grains are complicated and vary between 0° and 90° connections, how does one address the averaging problem of different-mode connection units?

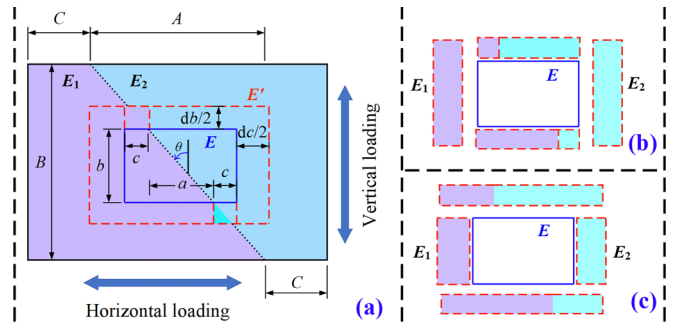


FIG. 2. Illustrations of the analytical method for calculating the modulus of a general inclined connection: (a) adding an infinitesimal layer on the inner blue rectangle to generate an increment dE ; and (b) SP and (c) PS connections for calculating E' .

2. As the elastic moduli of all the grains are different because of their varying orientations, how does one address the many-body connection problem?

For simplification, we have to make certain assumptions. First, these fundamental assumptions regarding the composite structure connection problem can be described as (i) strain compatibility between grains, (ii) perfect bonding at grain boundaries, and (iii) negligible elastic interactions between individual connection units (for detailed descriptions, see Refs. [29,30]). In addition, we assume that the grain orientation remains unchanged during the process of elastic deformation. This ensures that the elastic modulus of each grain remains constant in the computational process. Although the shear deformation induced by tensile or compressive stress can lead to changes in grain orientation, this phenomenon primarily occurs during plastic deformation [19,31]. During elastic deformation, the grain orientation remains largely constant, making such an assumption reasonable. Finally, let us suppose that the polycrystalline material contains only two kinds of orientations (called the two-body connection problem in this work), which are uniformly distributed among each other for structural macroscale homogeneity. Assuming that grain boundary planes are randomly located, the parallel and series connections should be only two special connection cases that are the upper and lower bounds of them, as shown in Figs. 1(b) and 1(c), and a more general connection mode should be with a random inclined angle θ ($0^\circ \leq \theta \leq 90^\circ$), as illustrated in Fig. 1(e). For the uniform structure containing a large number of random inclined connections, the 45° inclined connection may be regarded as an averaging approximation, as shown in Fig. 1(d). This treatment is a simplified solution to the first problem, i.e., the two-body connection problem. Based on these results, the many-body connection problem may be solved by analogy and extension methods, which is the solution to the second problem.

B. Calculating the modulus of a general inclined connection

For a general case of inclined connection, a rectangle composite with two right trapezoids of the same size is considered along different loading directions, as shown in Fig. 2, in which the moduli of the two right trapezoids are E_1 and E_2 ,

respectively, and the edge lengths of the three right-angle sides are $C + A$, B , and C , respectively. For an inner rectangle of the two-phase composite (the small rectangle with blue solid lines in Fig. 2), which is similar to the outer one, the modulus is designated as E . When a layer of two phases with infinitesimal thickness db on the top and bottom and $dc = (a + 2c)db/b$ on the two sides is added, as shown in Fig. 2, the modulus of the rectangle composite (framed by red dashed lines in Fig. 2) becomes $E' = E + dE$.

For the vertical loading case, there are two ways for evaluating the value of E' :

1. Let the inner blue rectangle first connect in series with the upper and lower red rectangles, using the Reuss equation to calculate the modulus E_{center} , and then connect in parallel with the red rectangles on both sides, and using the Voigt equation to calculate the modulus E' , as shown in Fig. 2(b). It should be noted that the upper and lower red rectangles are also composites with moduli that should be calculated first using the Voigt equation before the first connection. Here, this connection sequence is called the SP connection, which uses connection first in series and then in parallel.

2. Alternatively, let the inner blue rectangle first connect in parallel with the red rectangles on both sides, using the Voigt equation to calculate the modulus E_{center} , and then connect in series with the upper and lower red rectangles, and using the Reuss equation to calculate the modulus E' , as shown in Fig. 2(c). Accordingly, this connection sequence is called PS, which uses connection first in parallel and then in series.

As discussed in our previous work [30], these SP and PS connections should be the respective lower and upper bounds of the mixed modulus for the rectangle composite, and, consequently, the actual value for the modulus of the composite must be located between the two bounds. If it can be proved that, for the infinitesimal increments db and dc , the difference between the two bounds dE_{SP} and dE_{PS} also become infinitesimal so that the modulus E acquired by the two connection sequences converges into an identical value, this must be the real modulus for the rectangle composite. Therefore, in the following, we will prove the convergence of the two bounds for the modulus E and calculate its value analytically.

First, the case of SP connection under vertical loading is considered, as shown in Fig. 2(b). The moduli of the upper and lower rectangle composites (E_{up} and E_{low} , respectively) can be calculated using the Voigt equation:

$$E_{up} = E_1 f_1 + E_2(1 - f_1), E_{low} = E_2 f_1 + E_1(1 - f_1), \quad (2)$$

where $f_1 = c/(a + 2c)$.

And then these two rectangles are connected in series with a composite modulus of $E_{up/low}$, which is calculated by using the Reuss equation:

$$E_{up/low} = 2E_{up}E_{low}/(E_{up} + E_{low}). \quad (3)$$

Then, the modulus of the center region (called E_{center}) containing the upper rectangle, lower rectangle, and the blue rectangle can be calculated by using the Reuss equation:

$$E_{center} = E_{up/low}E/[E_{up/low}f_2 + E(1 - f_2)], \quad (4)$$

where $f_2 = b/(b + db)$.

The right and left rectangles are connected in parallel with a composite modulus of $E_{left/right}$, which is calculated by using the Voigt equation:

$$E_{left/right} = (E_1 + E_2)/2. \quad (5)$$

Finally, the modulus of the red region can be calculated by using the Voigt equation:

$$E' = E_{left/right}f_3 + E_{center}(1 - f_3), \quad (6)$$

where $f_3 = dc/(a + 2c + dc)$.

With combinations of Eqs. (2) through (6) and $dc = (a + 2c)db/b$, E' can be calculated, and then dE_{SP} can be expressed as

$$dE_{SP} = E' - E = \frac{F_1 db + F_2 (db)^2}{F_3 + F_4 db + F_5 (db)^2}, \quad (7)$$

where F_1, F_2, F_3, F_4 , and F_5 are the functions of a, b, c, E, E_1 , and E_2 . Ignoring the infinitesimal terms of high order, Eq. (7) can be written as

$$dE_{SP} = \frac{(E_1 + E_2)[a^2(E_1 E_2 - E^2) + c(a + c)((E_1 + E_2)^2 - 4E^2)]}{2b[aE_1 + c(E_1 + E_2)][aE_2 + c(E_1 + E_2)]} db. \quad (8)$$

Next, the case of the PS connection under vertical loading is considered, as shown in Fig. 2(c). The moduli of the upper and lower rectangle composites (called \bar{E}_{up} and \bar{E}_{low}) can be calculated by using the Voigt equation:

$$\bar{E}_{up} = E_1 f_4 + E_2(1 - f_4), \bar{E}_{low} = E_2 f_4 + E_1(1 - f_4), \quad (9)$$

where $f_4 = (dc/2 + c)/(a + 2c + dc)$.

And then the two rectangles are connected in series with a composite modulus of $\bar{E}_{up/low}$, which is calculated by using the Reuss equation:

$$\bar{E}_{up/low} = 2\bar{E}_{up}\bar{E}_{low}/(\bar{E}_{up} + \bar{E}_{low}). \quad (10)$$

The right and left rectangles are connected in parallel with a composite modulus of $\bar{E}_{left/right}$, which is calculated by using the Voigt equation:

$$\bar{E}_{left/right} = (E_1 + E_2)/2. \quad (11)$$

The modulus of the center region (called \bar{E}_{center}) containing the left rectangle, right rectangle, and the blue rectangle can be calculated by using the Voigt equation:

$$\bar{E}_{center} = \bar{E}_{left/right}f_5 + E(1 - f_5), \quad (12)$$

where $f_5 = dc/(a + 2c + dc)$.

Finally, the modulus of the red region can be calculated by using the Reuss equation:

$$E' = \bar{E}_{\text{up/low}} \bar{E}_{\text{center}} / [\bar{E}_{\text{center}} f_6 + \bar{E}_{\text{up/low}} (1 - f_6)], \quad (13)$$

where $f_6 = db/(b + db)$.

With combinations of Eqs. (9) through (13) and $dc = (a + 2c)db/b$, E' can be calculated, and then dE_{PS} can be obtained after ignoring the infinitesimal terms of high order:

$$dE_{\text{PS}} = \frac{(E_1 + E_2)[a^2(E_1 E_2 - E^2) + c(a + c)((E_1 + E_2)^2 - 4E^2)]}{2b[aE_1 + c(E_1 + E_2)][aE_2 + c(E_1 + E_2)]} db = dE_{\text{SP}}. \quad (14)$$

Here, we prove the modulus increments for SP and PS connections are the identical values after ignoring the infinitesimal terms of high order, which means this method is valid for the two-phase inclined connection problem. In Ref. [30], we obtained the elastic modulus of discrete composite structures by solving a differential equation regarding the elastic modulus. However, in this two-phase inclined connection problem, note that the red dashed rectangle is similar to the blue solid rectangle, as shown in Fig. 2(a), and thus it should satisfy $dE = 0$. Based on this condition, the modulus E can be derived from Eq. (14):

$$E_{\text{vertical}} = \frac{\sqrt{(E_1 + E_2)^2(r + r^2) + E_1 E_2}}{1 + 2r}, \quad (15)$$

where $r = \frac{c}{A}$.

In the same way, the modulus under horizontal loading can be obtained (see the Appendix), and it is expressed as

$$E_{\text{horizontal}} = \frac{E_1 E_2 (1 + 2r)}{\sqrt{(E_1 + E_2)^2(r + r^2) + E_1 E_2}}, \quad (16)$$

where $r = \frac{c}{A}$.

For the case of the general connection in Fig. 1, the composite modulus can be expressed as the function of θ . At $0 < \theta < 45^\circ$, the modulus can be obtained by substituting $r = [\cot(\theta) - 1]/2$ into Eq. (16). At $45^\circ < \theta < 90^\circ$, the modulus can be obtained by substituting $r = [\tan(\theta) - 1]/2$ into Eq. (15). Thus, the modulus can be written as

$$E(\theta) = \begin{cases} \frac{2E_1 E_2}{\tan(\theta) \sqrt{(E_1 + E_2)^2 \csc^2(\theta) - 2(E_1^2 + E_2^2)}}, & 0 < \theta < 45^\circ; \\ \sqrt{E_1 E_2}, & \theta = 45^\circ; \\ \frac{\sqrt{(E_1 + E_2)^2 \sec^2(\theta) - 2(E_1^2 + E_2^2)}}{2 \tan(\theta)}, & 45^\circ < \theta < 90^\circ. \end{cases} \quad (17)$$

According to the analysis in Sec. II A, we assume that the 45° inclined connection is an averaging approximation for the uniform structure containing a large number of random inclined connections. Thus, the elastic modulus of a polycrystalline material containing only two crystal orientations can be approximately calculated by

$$E = \sqrt{E_1 E_2}. \quad (18)$$

As shown in Eq. (18), in fact, the composite modulus of the two-body connection is the geometric mean of their moduli. For the many-body connection problem, we assume that the composite modulus can also be approximately calculated by the geometric mean, and thus the elastic modulus of a polycrystalline material with multiple orientations can be

reasonably derived:

$$E_{\text{poly}} = \left(\prod_{i=1}^n E_i \right)^{\frac{1}{n}}. \quad (19)$$

Interestingly, the formula for calculating the elastic modulus of a polycrystalline material is obtained by the current method, which is the same as the existing work in Ref. [25].

III. VERIFICATION

In this section, the theoretical solutions presented in Sec. II B will be verified step by step. First, the two-dimensional solution of the inclined-connection composite modulus, i.e., Eq. (17), is compared with the results obtained by the finite element method (FEM). Second, the formula for calculating the elastic modulus of polycrystalline materials, i.e., Eq. (19), is verified by the FEM, and then the formula is further verified by the existing experimental results [26].

At first, two-dimensional finite element models are established by ABAQUS [32] to examine the correctness of Eq. (17), and the compared results are shown in Fig. 3. The elastic moduli of the two components are 50 GPa and 150 GPa, respectively. A uniform tensile displacement load is applied to measure the composite modulus. The results show that the composite modulus calculated by our proposed method is consistent with the value by the FEM, which verifies the solution in Eq. (17).

To verify this method further, three-dimensional polycrystalline finite element models are established, as shown in

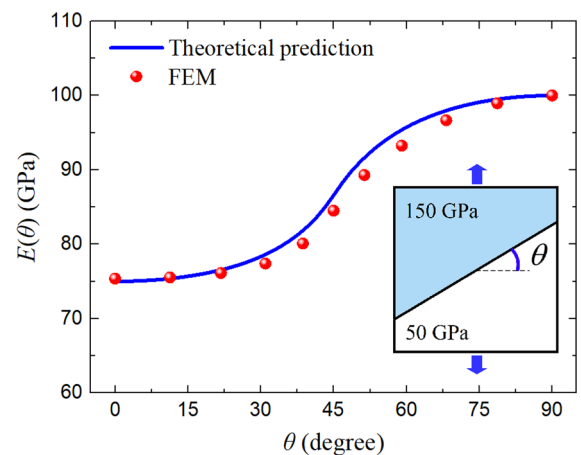


FIG. 3. Comparison of the composite modulus for inclined connections between the present method and FEM.

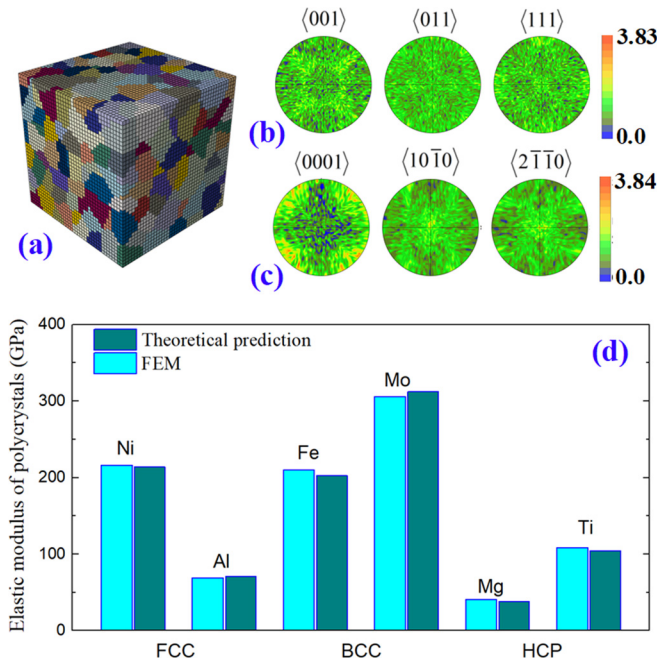


FIG. 4. Comparison between the theoretical prediction [Eq. (19)] and the FEM. (a) The finite element model of polycrystals. (b) The crystal orientation pole figure for the cubic structures (fcc and bcc). (c) The crystal orientation pole figure for the hcp structure. (d) Comparison of the elastic modulus between the theoretical calculations and the finite element simulations.

Fig. 4(a). To validate the generality of our proposed method, we selected six kinds of metals corresponding to three kinds of typical crystal structures—namely, fcc, bcc, and hcp crystal structures. The finite element model has a size of $40\ \mu\text{m} \times 40\ \mu\text{m} \times 40\ \mu\text{m}$ and consists of 410 grains with random orientations, as shown in Figs. 4(b) and 4(c). Figure 4(b) displays the crystal orientation pole figure for fcc and bcc polycrystals, while Fig. 4(c) shows the pole figures for hcp polycrystals. The elastic constants are taken as shown in Table I. The comparison between the theoretical prediction and the FEM is shown in Fig. 4(d), and it is demonstrated that the two sets of results agree well with each other, indicating the feasibility of the theoretical method proposed in this work.

Next, the geometric mean formula [Eq. (19)] is compared with the reported experimental results [26]. The testing material was a high-strength low-alloy steel (H480LA), and its anisotropic microstructures and moduli were generated by linear flow splitting, which is a severe plastic deformation technique. To describe the anisotropy conveniently, a

TABLE I. The elastic constants of metals (unit: GPa).

Materials	C_{11}	C_{12}	C_{44}	C_{13}	C_{33}
Ni [11]	246.5	147.3	124.7		
Al [11]	108.2	61.3	28.5		
Fe [11]	228	132	116.5		
Mo [11]	460	176	110		
Mg [33]	59.4	25.6	16.4	21.4	61.6
Ti [34]	162.2	91.8	46.7	68.8	180.5

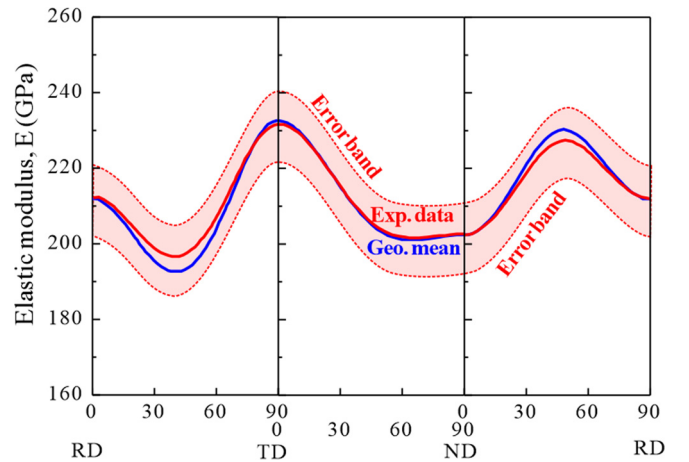


FIG. 5. Comparison of the elastic modulus between the geometric (Geo.) mean formula (blue line) and experimental measurements (red line) [26].

coordinate system was defined. The three coordinate axes were the rolling direction (RD), the transverse direction (TD), and the normal direction (ND). The comparison between the analytical formula [Eq. (19)] and the reported experimental results is shown in Fig. 5. It shows that there is the highest deviation between the experimental data and the predicted results at about 45° between RD and TD as well as ND and RD. This is due to our approximation of grain connectivity using the 45° inclined connection. The experimental materials were obtained using a severe plastic deformation technique, resulting in the elongated grain structures [26]. For elongated grains, when calculating the elastic modulus in the direction of grain elongation, the grain connections tend to be in parallel. Conversely, when calculating the elastic modulus in the direction perpendicular to the grain elongation, the grain connections tend to be in series. Hence, this would produce a larger error. Overall, there is only a little difference between the predicted results by the geometric mean formula and experimental measurements, indicating that the analytical expressions derived in this work are valid.

IV. APPLICATION

To obtain the elastic modulus of polycrystalline materials more easily, EBSD-based software has been developed called orientation-based elasticity calculation, or OBEC. The elastic modulus of single crystals is anisotropic, and it is described by combining the basal elastic stiffness matrix and crystal orientations [11,27]. The elastic stiffness matrix of single-crystal materials is easily obtained by the related handbook. The elastic modulus of single crystals along an arbitrary orientation is usually calculated by rotating the stiffness matrix. With our software, the orientations of polycrystals are given by EBSD, and then each data point is regarded as a single crystal. Thus, the elastic modulus of each single crystal can be calculated by the basal elastic stiffness matrix and rotation matrix. Finally, the elastic modulus of the polycrystalline material is calculated using Eq. (19). The outcome interfaces of the developed software are shown in Fig. 6(a). As long as an EBSD file of a polycrystal is loaded, the elastic modulus

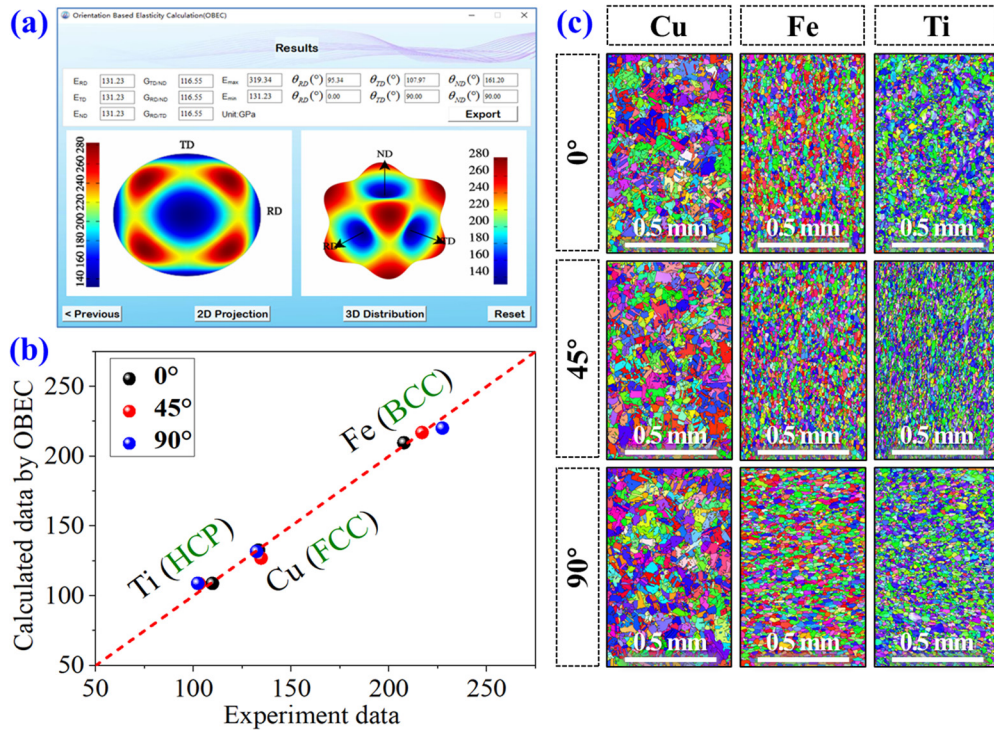


FIG. 6. (a) Outcome interfaces of the developed software. (b) EBSD images of three kinds of typical crystalline metals with three typical directions. (c) Comparison between the predicted results by our software and the experimental measurements (unit: GPa).

of the polycrystalline material can be given by the developed software.

In order to examine the feasibility of the software, three kinds of metals with common annealed crystalline structures (fcc, bcc, and hcp) are selected, and their elastic moduli calculated by the software based on the EBSD data [Fig. 6(b)] are compared with the corresponding experimental results using the free resonant vibration method according to Chinese standard GB/T2105-91, using samples 3 mm in diameter and 60 mm in length. The comparison results are shown in Fig. 6(c). It is apparent that the values obtained by the software are well consistent with the corresponding experimental data, which verifies the practicability of the software. Note that the software is still valid to predict the elastic moduli of fcc, bcc, and hcp metals with multiphases. For multiphase materials, the different phases possess distinct elastic moduli, akin to the variation in elastic moduli among different grains in polycrystalline materials. If the dimensions of the reinforcing phases are on the micron scale, the volume fraction occupied by the phase boundaries is exceedingly small. Therefore, neglecting the influence of this factor has minimal impact on the prediction for the elastic modulus of multiphase materials.

In Sec. II A, we assume that the 45° inclined connection unit is an averaging approximation for polycrystalline materials containing a large number of randomly inclined connections between adjacent grains. Based on this assumption, we derive the elastic modulus of polycrystals. However, this assumption is limited by the shape of grains. The 45° inclined connection unit is not a parallel or series connection, but rather an intermediate connection mode. For polycrystalline materials consisting of elongated grains, the connection mode

is closer to the parallel connection when the tensile direction is along the elongated direction of grains, and is closer to the series connection when the tensile direction is perpendicular to the elongated direction of grains. In this case, using the 45° inclined connection unit as an averaging approximation is invalid. However, for materials consisting of equiaxed grains, the assumption is reasonable. Additionally, the effect of the grain-boundary phase on the elastic modulus of polycrystals is neglected in our calculation. In fact, the volume fraction of grain boundaries increases sharply with decreasing grain size, and it cannot be neglected in nanocrystalline materials [19,20]. For example, the volume fraction of grain boundaries is less than 5% when grain size is 100 nm, while it reaches about 15% when grain size is 20 nm [19,20]. Based on these analyses, the formulae and developed software in this work should be valid for predicting the elastic modulus of coarse-grained, fine-grained, and ultrafine-grained materials consisting of equiaxed grains, but not for elongated grains or nanocrystalline materials.

V. CONCLUSION

The elastic modulus of a polycrystalline material is a comprehensive effect of the elastic deformation responses of all individual grains. To tackle this complex problem, we simplified it into two subproblems. First, based on the proposed LLI method, we addressed the complex intergranular connections by averaging the connections between grains into the 45° inclined connection unit. Second, we dealt with the multibody connection problem by deriving a geometric mean formula to calculate the elastic modulus of multibody connections. Furthermore, we established two-dimensional bicrystal

models and three-dimensional polycrystal models to validate our theoretical derivation using the FEM. By comparing the theoretical results with the existing experimental data, we further confirmed the correctness of our theoretical derivation. Based on the derived formulae, we developed software for predicting the elastic modulus of polycrystalline materials based on EBSD data. This software can quickly and accurately predict the elastic modulus of polycrystalline materials by uploading an EBSD file. In summary, this work theoretically derived the elastic modulus of complex multibody connections, and realized the prediction of the elastic modulus of polycrystalline materials using a simple method/software.

The raw/processed data required to reproduce these findings will be made available on request.

ACKNOWLEDGMENTS

This work is financially supported by the Youth Innovation Promotion Association Chinese Academy of Sciences (CAS) (Grant No. 2021192), the National Natural Science Foundation of China (Grants No. 52322105, No. 52130002, No. 52271121, No. 52321001, No. 52001153, No. 52261135634, and No. U2241245), the IMR Innovation Fund (Grant No. 2023-ZD01), the K. C. Wong Education Foundation (Grant No. GJTD-2020-09), the Shi Changxu Innovation Center for Advanced Materials, and the Joint Research Project between the CAS (Grant No. 172GJHZ2022030MI).

APPENDIX: THE DERIVATION OF THE ELASTIC MODULUS OF A GENERAL INCLINED CONNECTION UNIT UNDER HORIZONTAL LOADING

Here, the solution of the elastic modulus of a general inclined connection unit under horizontal loading is presented. First, the case in Fig. 2(b) under horizontal loading

is considered. The moduli of the upper and lower rectangle composites— E_{up-A} and E_{low-A} , respectively, can be calculated using the Reuss equation:

$$E_{up-A} = \frac{E_1 E_2}{E_1(1 - f_1) + E_2 f_1}, E_{low-A} = \frac{E_1 E_2}{E_2(1 - f_1) + E_1 f_1}, \tag{A1}$$

where $f_1 = c/(a + 2c)$.

And then the two rectangles are connected in parallel with a composite modulus of $E_{up-A/low-A}$, which is calculated using the Voigt equation:

$$E_{up-A/low-A} = (E_{up-A} + E_{low-A})/2. \tag{A2}$$

Then, the modulus of the center region $E_{center-A}$ containing the upper rectangle, lower rectangle, and the blue rectangle can be calculated using the Voigt equation:

$$E_{center-A} = E_{up-A/low-A}(1 - f_2) + E f_2, \tag{A3}$$

where $f_2 = b/(b + db)$.

The right and left rectangles are connected in series with a composite modulus of $E_{left-A/right-A}$, which is calculated using the Reuss equation:

$$E_{left-A/right-A} = 2E_1 E_2 / (E_1 + E_2). \tag{A4}$$

Finally, the modulus of the red region can be calculated using the Reuss equation:

$$E' = \frac{E_{left-A/right-A} E_{center-A}}{E_{left-A/right-A}(1 - f_3) + E_{center-A} f_3}, \tag{A5}$$

where $f_3 = dc/(a + 2c + dc)$

Combinations of Eqs. (A1) through (A5) and $dc = (a + 2c)db/b$, E' can be calculated, and then dE_{PS-A} can be expressed as

$$dE_{PS-A} = E' - E = \frac{F_{1-A}db + F_{2-A}(db)^2 + F_{3-A}(db)^3}{F_{4-A} + F_{5-A}db + F_{6-A}(db)^2 + F_{7-A}(db)^3}, \tag{A6}$$

where F_{1-A} , F_{2-A} , F_{3-A} , F_{4-A} , F_{5-A} , F_{6-A} , and F_{7-A} are the functions of a , b , c , E , E_1 , and E_2 . Ignoring the infinitesimal terms of high order and letting $dE_{PS-A} = 0$, the modulus can be obtained:

$$E_{horizontal} = \frac{(a + 2c)E_1 E_2}{\sqrt{[aE_1 + c(E_1 + E_2)][aE_2 + c(E_1 + E_2)]}}. \tag{A7}$$

Similarly, the case in Fig. 2(c) under horizontal loading can be calculated with the SP connection mode, and the elastic modulus in this case is same as Eq. (A7)

[1] G. López-Polín, C. Gómez-Navarro, V. Parente, F. Guinea, M. I. Katsnelson, F. Perez-Murano, and J. Gómez-Herrero, Increasing the elastic modulus of graphene by controlled defect creation, *Nat. Phys.* **11**, 26 (2015).

[2] A. Haglund, M. Koehler, D. Catoor, E. P. George, and V. Keppens, Polycrystalline elastic moduli of a high-entropy alloy at cryogenic temperatures, *Intermetallics* **58**, 62 (2015).

[3] D. Ma, A. Stoica, X.-L. Wang, Z. Lu, B. Clausen, and D. Brown, Elastic moduli inheritance and the weakest link in bulk metallic glasses, *Phys. Rev. Lett.* **108**, 085501 (2012).

[4] D. Lee, S. G. Kim, S. Hong, C. Madrona, Y. Oh, M. Park, N. Komatsu, L. W. Taylor, B. Chung, J. Kim *et al.*, Ultra-high strength, modulus, and conductivity of graphitic fibers by macromolecular coalescence, *Sci. Adv.* **8**, eabn0939 (2022).

- [5] M. D. Norman, S. A. Ferreira, G. M. Jowett, L. Bozec, and E. Gentleman, Measuring the elastic modulus of soft culture surfaces and three-dimensional hydrogels using atomic force microscopy, *Nat. Protoc.* **16**, 2418 (2021).
- [6] S. Mathesan and D. Mordehai, Size-dependent elastic modulus of nanoporous Au nanopillars, *Acta Mater.* **185**, 441 (2020).
- [7] M. Tane, H. Okuda, and F. Tanaka, Nanocomposite microstructures dominating anisotropic elastic modulus in carbon fibers, *Acta Mater.* **166**, 75 (2019).
- [8] C. Tromas, J.-C. Stinville, C. Templier, and P. Villechaise, Hardness and elastic modulus gradients in plasma-nitrided 316L polycrystalline stainless steel investigated by nanoindentation tomography, *Acta Mater.* **60**, 1965 (2012).
- [9] Z. Chen, X. Wang, F. Giuliani, and A. Atkinson, Microstructural characteristics and elastic modulus of porous solids, *Acta Mater.* **89**, 268 (2015).
- [10] G. Vazquez, P. Singh, D. Saucedo, R. Couperthwaite, N. Britt, K. Youssef, D. D. Johnson, and R. Arróyave, Efficient machine-learning model for fast assessment of elastic properties of high-entropy alloys, *Acta Mater.* **232**, 117924 (2022).
- [11] M. A. Meyers and K. K. Chawla, *Mechanical Behavior of Materials* (Cambridge University Press, Cambridge, 2008).
- [12] D. Hull and D. J. Bacon, *Introduction to Dislocations* (Elsevier, Amsterdam, 2011).
- [13] P. Zhang and Z.-F. Zhang, Getting tougher in the ultracold, *Science* **378**, 947 (2022).
- [14] Y. Wang, M. Chen, F. Zhou, and E. Ma, High tensile ductility in a nanostructured metal, *Nature (London)* **419**, 912 (2002).
- [15] T. Fang, W. Li, N. Tao, and K. Lu, Revealing extraordinary intrinsic tensile plasticity in gradient nano-grained copper, *Science* **331**, 1587 (2011).
- [16] P. M. Ajayan, L. S. Schadler, and P. V. Braun, *Nanocomposite Science and Technology* (Wiley, Weinheim, 2006).
- [17] L. Lu, X. Chen, X. Huang, and K. Lu, Revealing the maximum strength in nanotwinned copper, *Science* **323**, 607 (2009).
- [18] R. Valiev, Y. Estrin, Z. Horita, T. Langdon, M. Zehetbauer, and Y. Zhu, Fundamentals of superior properties in bulk nanoSPD materials, *Mater. Res. Lett.* **4**, 1 (2016).
- [19] I. Ovid'ko, R. Valiev, and Y. Zhu, Review on superior strength and enhanced ductility of metallic nanomaterials, *Prog. Mater. Sci.* **94**, 462 (2018).
- [20] M. A. Meyers, A. Mishra, and D. J. Benson, Mechanical properties of nanocrystalline materials, *Prog. Mater. Sci.* **51**, 427 (2006).
- [21] M. Kamaya, A procedure for estimating Young's modulus of textured polycrystalline materials, *Int. J. Solids Struct.* **46**, 2642 (2009).
- [22] W. Voigt, *Lehrbuch der Kristallphysik* (BG Teubner, Leipzig, 1928).
- [23] A. Reuss, Berechnung der fließgrenze von mischkristallen auf grund der plastizitätsbedingung für einkristalle, *Z. Angewandte Mathematik Mechanik* **9**, 49 (1929).
- [24] R. Hill, The elastic behaviour of a crystalline aggregate, *Proc. Phys. Soc. London Sect. A* **65**, 349 (1952).
- [25] U. F. Kocks, C. N. Tomé, and H.-R. Wenk, *Texture and Anisotropy: Preferred Orientations in Polycrystals and Their Effect on Materials Properties* (Cambridge University Press, Cambridge, 2000).
- [26] J. Niehuesbernd, C. Müller, W. Pantleon, and E. Bruder, Quantification of local and global elastic anisotropy in ultrafine grained gradient microstructures, produced by linear flow splitting, *Mater. Sci. Eng. A* **560**, 273 (2013).
- [27] J. Den Toonder, J. Van Dommelen, and F. Baaijens, The relation between single crystal elasticity and the effective elastic behaviour of polycrystalline materials: Theory, measurement and computation, *Model. Sim. Mater. Sci. Eng.* **7**, 909 (1999).
- [28] Z. Hashin and S. Shtrikman, A variational approach to the theory of the elastic behaviour of polycrystals, *J. Mech. Phys. Solids* **10**, 343 (1962).
- [29] K. S. Ravichandran, Elastic properties of two-phase composites, *J. Am. Ceram. Soc.* **77**, 1178 (1994).
- [30] Z. J. Zhang, Y. K. Zhu, P. Zhang, Y. Y. Zhang, W. Pantleon, and Z. F. Zhang, Analytic approximations for the elastic moduli of two-phase materials, *Phys. Rev. B* **95**, 134107 (2017).
- [31] J. Munoz-Saldana, G. Schneider, and L. Eng, Stress induced movement of ferroelastic domain walls in BaTiO₃ single crystals evaluated by scanning force microscopy, *Surf. Sci.* **480**, L402 (2001).
- [32] H. Hibbitt, B. Karlsson, and E. Sorensen, *ABAQUS, ABAQUS/Standard User's Manual*, ver. 6.5 (2004).
- [33] J. Zhang and S. P. Joshi, Phenomenological crystal plasticity modeling and detailed micromechanical investigations of pure magnesium, *J. Mech. Phys. Solids* **60**, 945 (2012).
- [34] A. Alankar, P. Eisenlohr, and D. Raabe, A dislocation density-based crystal plasticity constitutive model for prismatic slip in α -titanium, *Acta Mater.* **59**, 7003 (2011).